

Cover Tree Bayesian Reinforcement Learning

Nikolaos Tziortziotis

Christos Dimitrakakis

Konstantinos Blekas

November 16, 2016

Abstract

This paper proposes an online tree-based Bayesian approach for reinforcement learning. For inference, we employ a generalised context tree model. This defines a distribution on multivariate Gaussian piecewise-linear models, which can be updated in closed form. The tree structure itself is constructed using the cover tree method, which remains efficient in high dimensional spaces. We combine the model with Thompson sampling and approximate dynamic programming to obtain effective exploration policies in unknown environments. The flexibility and computational simplicity of the model render it suitable for many reinforcement learning problems in continuous state spaces. We demonstrate this in an experimental comparison with least squares policy iteration.

1 Introduction

In reinforcement learning, an agent must learn how to act in an unknown environment from limited feedback and delayed reinforcement. In this paper, we assume that the environment is a fully observable discrete-time Markov, with state space $\mathcal{S} \subset \mathbb{R}^m$. At time t , the agent observes the current environment state $s_t \in \mathcal{S}$, takes an action a_t from a discrete set \mathcal{A} , and observes a reward $r_t \in \mathbb{R}$. The goal of the agent is to maximise its expected utility:

$$\max_{\pi} \mathbb{E}_{\mu}^{\pi} U = \max_{\pi} \mathbb{E}_{\mu}^{\pi} \sum_{t=0}^{\infty} \gamma^t r_t, \quad \gamma \in [0, 1], \quad (1.1)$$

where the value of the expectation depends on the agent's policy π and the environment μ , while γ is

a discount factor such that rewards further into the future are less important than immediate rewards. Well-known dynamic programming algorithms can be used to find the optimal policy in the discrete-state case [34], while many approximate algorithms exist for continuous environments [7]. In this case the optimal policies are generally memoryless.

However, since the environment μ is unknown, the maximisation is not well defined. In the Bayesian framework for reinforcement learning, this problem is alleviated by performing the maximisation conditioned on the agent's belief about the true environment μ .

1.1 Bayesian reinforcement learning

The main assumption in Bayesian reinforcement learning is that the environment μ lies in a given set of environments \mathcal{M} . In addition, the agent must select a subjective prior distribution $p(\mu)$ which encodes its belief about which environments are most likely. The Bayes-optimal expected utility for p is:

$$U_p^* \triangleq \max_{\pi} \mathbb{E}_p^{\pi} U = \max_{\pi} \int_{\mathcal{M}} (\mathbb{E}_{\mu}^{\pi} U) dp(\mu). \quad (1.2)$$

Unlike the known μ case, the optimal policy may not be memoryless, as our belief changes over time. This makes the optimisation over the policies significantly harder [23]. While many interesting approximate Bayesian approaches exist [4, 16, 28, 33, 40, 41], this paper will focus on the simple idea of Thompson sampling [38], which has been shown to be near-optimal in certain settings [29].

The second problem in Bayesian reinforcement learning is the choice of prior. The main contribution of this paper is the introduction of a prior over

piecewise-linear multivariate Gaussian models. This is based on a construction of a context tree model, using a cover tree structure, which defines a conditional distribution on local linear Bayesian multivariate models. Since inference for the model is closed form, the resulting algorithm is very efficient.

1.2 Related work

One component in our model is the *context tree*. Context trees were introduced in [42] for sequential prediction [see 6, for an overview]. In this model, a distribution of variable order Markov models for binary sequences is constructed, where the tree distribution is defined through context-dependent weights (for probability of an edge being part of the tree) and Beta distributions (for predicting the next observation). Many reinforcement learning approaches based on such trees have been proposed, but have mainly focused on the discrete partially observable case [17, 22, 26, 40].¹ However, tree structures can generally be used to perform Bayesian inference in a number of other domains [31, 32, 43].

Another component in our model is the Bayesian multivariate linear model at each node of the tree. Other approaches incorporating linear models include [37], which proves mistake bounds on reinforcement learning algorithms using online linear regression, and [1] who use separate linear models for each dimension. Another related approach in terms of the model structure is [13], which partitions the space into *types* and estimates a simple additive model for each type.

Linear-Gaussian models are naturally generalised by Gaussian processes (GP). Some examples of GP in reinforcement learning include [19, 20, 35], which focused on a model-predictive approach, while that of Engel et al. [24] employed GPs for expected utility estimation. A general difficulty with GPs is the computational complexity, which our tree-structured model avoids. A problem specific to the cited model-based GP-RL approaches is that they employ the

¹We note that another important work in tree-based reinforcement learning, though not directly related to ours, is that of [25], which uses trees for expected utility rather than model estimation.

marginal distribution within the dynamic programming step, which is only a heuristic (c.f. eqs. 1.2, 2.11). Finally, each output dimension of the model is treated with an independent GP, which many not make good use of the data. Although methods for efficient dependent GPs exist [3], they have not yet been applied to reinforcement learning.

To make decisions using our model, we employ Thompson sampling [38, 39]. This avoids the computational complexity of building augmented MDP models [4, 5, 16], Monte-Carlo tree search [40], sparse sampling [41], or creating lower bounds on the Bayes-optimal value function [33]. Nevertheless, it has been shown to perform quite well [2, 38] for bandit problems. However, its theoretical performance in general reinforcement learning is currently unknown.

1.3 Our contribution

Our approach is based on three main ideas. Firstly, we employ a cover tree model [10] to create a set of partitions of the state space. Secondly, we construct an efficient non-parametric Bayesian conditional density estimator on the cover tree structure. This is a context tree, which is endowed with a linear Bayesian model at each node. This can be used to estimate the dynamics of the underlying environment. Inference very efficient, even though we model all output dimensions jointly. Finally, by taking a sample from the posterior distribution, we end up with a piecewise linear Gaussian model of the dynamics. We use this to obtain trajectories of simulated experience. This can then be used to perform approximate dynamic programming (ADP) in order to select a policy.

Overall, our approach is very efficient. The posterior calculation and prediction is fully conjugate and can be performed in logarithmic time. Sampling is anytime and linear in the worst case. These properties are in contrast to other non-parametric approaches for reinforcement learning such as Gaussian processes. The most computationally heavy step of our algorithm is ADP. However, once a policy is calculated, the next action to be taken can be calculated in logarithmic time.

2 Cover Tree Bayesian Reinforcement Learning

The main idea of cover tree Bayesian reinforcement learning (CTBRL) is to construct a cover tree from the observations, simultaneously inferring a conditional probability density on the same structure. This density can be seen as a distribution over piecewise linear Gaussian densities. By taking a sample from this distribution, we acquire a specific model of the environment, which we can use to find an approximately optimal policy. The greatest advantage of the model is that the cover tree structure is efficient and flexible, and that its posterior distribution can be computed in closed form. Finally, we have a large choice over possible approximate dynamic programming methods.

More specifically, our algorithm works as follows. We take new observations using some previously chosen policy, while growing the tree as necessary and updating the posterior parameters of the tree and the local model in each relevant tree node. To calculate a new policy at time t , we sample a tree μ_k from the current posterior $p_t(\mu)$. This tree corresponds to a piecewise-linear model. We draw a large number of rollout trajectories from μ_k using an arbitrary exploration policy, starting from a uniform state distribution. These trajectories are used to estimate a near-optimal policy π_k using approximate dynamic programming.

An overview of the algorithm is given in pseudocode in Alg. 1. We now explain the algorithm in detail. First, we give an overview of the cover tree structure on which the context tree model is built. Then we show how to perform inference on the context tree, while section 2.3 describes the multivariate model used in each node of the context tree. Thompson sampling and the approximate dynamic method used are described in Sec. 2.4 and 2.5 respectively, while the overall complexity of the algorithm is discussed in Sec. 2.7.

Algorithm 1 CTBRL overview

```

 $k = 0, \pi_0 = \text{Unif}(\mathcal{A})$ , prior  $p_0$  on  $\mathcal{M}$ .
for  $t = 1, \dots, T$  do
  if episode-end then
     $k := k + 1$ .
    Sample model  $\mu_k \sim p_t(\mu)$ .
    Calculate policy  $\pi_k \approx \arg \max_{\pi} \mathbb{E}_{\mu, \pi} U$ .
  end if
  Observe state  $\mathbf{s}_t$ .
  Take action  $a_t \sim \pi_k(\cdot | \mathbf{s}_t)$ .
  Observe next state  $\mathbf{s}_{t+1}$ , reward  $r_{t+1}$ .
  Insert  $\mathbf{s}_t$  in the tree  $\mathcal{T}_{a_t}$ .
  Update posterior  $p_{t+1}(\mu) = p_t(\mu | \mathbf{s}_{t+1}, \mathbf{s}_t, a_t)$ .
end for

```

2.1 The cover tree structure

To construct a cover tree \mathcal{T} we require a set of points $D_t = \{\mathbf{z}_1, \dots, \mathbf{z}_t\}$, with $\mathbf{z}_i \in \mathcal{Z}$, a metric ψ and a constant $\zeta > 1$. The i -th tree node corresponds to the point $\mathbf{x}_{[i]}$ in this set. The nodes are arranged in *levels*, with each node being replicated in multiple levels. Thus, a point corresponds to multiple tree nodes, but at most one point at the same level. Let G_n denote the set of points corresponding to the nodes at level n of the tree and $\mathcal{C}(i)$ the corresponding set of children. If $i \in G_n$ then the level of i is $\ell(i) = n$. The tree has the following properties:

1. $G_n \subset G_{n-1}$.
2. For any $i, j \in G_n$, $\psi(\mathbf{x}_{[i]}, \mathbf{x}_{[j]}) > \zeta^n$.
3. If $i \in G_{n-1}$ then there exists a unique $j \in G_n$ such that $\psi(\mathbf{x}_{[i]}, \mathbf{x}_{[j]}) \leq \zeta^n$ and $i \in \mathcal{C}(j)$.

Thus, siblings at a particular level are guaranteed to be well-separated, while a child is guaranteed to be close to its parent. This is an important property, which directly gives rise to the theoretical guarantees given by the cover tree structure.

Reduced tree. As the formal definition of the cover tree duplicates nodes, in practice we use the *explicit representation* [see 10, Sec. 2 for more details]. This reduces the tree by only considering the top-most node in the tree corresponding to a point.

We denote this *reduced tree* by $\hat{\mathcal{T}}$. The *depth* $d(i)$ of node $i \in \hat{\mathcal{T}}$ is equal to its number of ancestors, with the root node having a depth of 0. After t observations, the set of nodes containing a point \mathbf{z} , is:

$$G_t(\mathbf{z}) \triangleq \left\{ i \in \hat{\mathcal{T}} \mid \mathbf{z} \in B_i \right\}, \quad (2.1)$$

where $B_i = \{ \mathbf{z} \in \mathcal{Z} \mid \psi(\mathbf{x}_{[i]}, \mathbf{z}) \leq \zeta^{\ell(i)} \}$ is the neighbourhood of i . Then $G_t(\mathbf{z})$ forms a path in the tree, as each node only has one parent, and can be discovered in logarithmic time through the **Find-Nearest** function [10, The. 5].

Each node $i \in G_t(\mathbf{z})$ is associated with a particular Bayesian multivariate model. The main problem is how to update the individual models and how to combine them. Fortunately, a closed form solution exists due to the tree structure.

2.2 Context tree inference

We now use the cover tree structure to define a *context tree*, which can be used for probabilistic inference. For each action $a \in \mathcal{A}$, we create a different reduced tree $\hat{\mathcal{T}}_a$, over the state space, i.e. $\mathcal{Z} = \mathcal{S}$, and using the Manhattan distance, i.e. $\psi(\mathbf{s}, \mathbf{s}') = \|\mathbf{s} - \mathbf{s}'\|_1$.

As with other tree models [22, 27, 32, 42], our model makes predictions by marginalising over a set of simpler models. Each node in the context tree is called a *context*, and each context is associated with a specific local model. At time t , given an observation $\mathbf{s}_t = \mathbf{s}$ and an action $a_t = a$, we calculate the marginal (predictive) density p_t of the next observation:

$$p_t(\mathbf{s}_{t+1} \mid \mathbf{s}_t, a_t) = \sum_{c_t} p_t(\mathbf{s}_{t+1} \mid \mathbf{s}_t, c_t) p_t(c_t \mid \mathbf{s}_t, a_t), \quad (2.2)$$

where we use the symbol p_t throughout for notational simplicity to denote marginal distributions from our posterior at time t . Here, c_t is such that if $p_t(c_t = i \mid \mathbf{s}_t, a_t) > 0$, then the current state is within the neighbourhood of i -th node of the cover tree, i.e. $\mathbf{s}_t \in B_i$. Each component density $p_t(\mathbf{s}_{t+1} \mid \mathbf{s}_t, c)$ corresponds to a linear Bayesian model, which we describe in the next section.

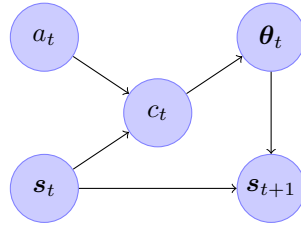


Figure 1: The simplified context tree graphical model.

The graphical structure of the model defined on the cover tree is shown in simplified form in Fig. 1. The context at time t depends only on the current state and action \mathbf{s}_t, a_t . The context corresponds to a particular local model with parameter θ_t , which defines the conditional distribution.

The probability distribution $p_t(c_t \mid \mathbf{s}_t, a_t)$ is defined as the probability of stopping at the i -th context, when performing a walk from the leaf node containing the current observation towards the root, stopping at the j -th node with probability $w_{j,t}$ along the way:

$$p_t(c_t = i \mid \mathbf{s}_t, a_t) = w_{i,t} \prod_{j \in \mathcal{D}(i)} (1 - w_{j,t}), \quad (2.3)$$

where $\mathcal{D}(i)$ are the descendants of i and $w_{0,t} = 1$. The stopping probability parameters can be updated in closed form [21] via Bayes' theorem:

$$w_{i,t+1} = \frac{p_t(\mathbf{s}_{t+1} \mid \mathbf{s}_t, c_t = i) w_{i,t}}{p_t(\mathbf{s}_{t+1} \mid \mathbf{s}_t, c_t \in \mathcal{D}(i))}. \quad (2.4)$$

It is easy to see that the denominator in the above equation can be calculated recursively via:

$$p_t(\mathbf{s}_{t+1} \mid \mathbf{s}_t, c_t \in \{i\} \cup \mathcal{D}(i)) = w_{i,t} p_t(\mathbf{s}_{t+1} \mid \mathbf{s}_t, c_t = i) + (1 - w_{i,t}) p_t(\mathbf{s}_{t+1} \mid \mathbf{s}_t, c_t \in \mathcal{D}(i)). \quad (2.5)$$

The weight parameter is initialised to $2^{-d(i)}$. The only remaining question is how to calculate the individual predictive marginal distributions for each context i . In this paper, we associate a linear Bayesian model with each context, which provides this distribution.

2.3 The linear Bayesian model

In our model we assume that, given $c_t = i$, the next state \mathbf{s}_{t+1} is given by a linear transformation of the current state and additive noise $\varepsilon_{i,t}$:

$$\mathbf{s}_{t+1} = \mathbf{A}_i \mathbf{x}_t + \varepsilon_{i,t}, \quad \mathbf{x}_t \triangleq \begin{pmatrix} \mathbf{s}_t \\ 1 \end{pmatrix}, \quad (2.6)$$

where \mathbf{x}_t is the current state vector augmented by a unit basis. In particular, each context models the dynamics via a Bayesian multivariate linear-Gaussian model. For each i -th context, there is a different (unknown) parameter pair $(\mathbf{A}_i, \mathbf{V}_i)$ where \mathbf{A}_i is the *design* matrix and \mathbf{V}_i is the *covariance* matrix. Then the next state distribution is:

$$\mathbf{s}_{t+1} \mid \mathbf{x}_t = \mathbf{x}, c_t = i \sim \mathcal{N}(\mathbf{A}_i \mathbf{x}, \mathbf{V}_i). \quad (2.7)$$

Thus, the parameters $\boldsymbol{\theta}_t$ which are abstractly shown in Fig. 1 correspond to the two matrices \mathbf{A}, \mathbf{V} . Let us now define the conditional distribution of these matrices given $c_t = i$.

We can model our uncertainty about these parameters with an appropriate prior distribution p_0 . In fact, a conjugate prior exists in the form of the *matrix inverse-Wishart normal* distribution. In particular, given \mathbf{V}_i , the distribution for \mathbf{A}_i is matrix-normal, while the marginal distribution of \mathbf{V}_i is inverse-Wishart, that is:

$$\mathbf{A}_i \mid \mathbf{V}_i = \mathbf{V} \sim \mathcal{N}(\mathbf{A}_i \mid \underbrace{\mathbf{M}, \mathbf{C}}_{\text{prior parameters}}, \mathbf{V}) \quad (2.8)$$

$$\mathbf{V}_i \sim \mathcal{W}(\mathbf{V}_i \mid \underbrace{\mathbf{W}, n}_{\text{prior parameters}}). \quad (2.9)$$

Here \mathcal{N} is the prior on design matrices, which has a matrix-normal distribution, conditional on the covariance and two prior parameters: \mathbf{M} , which is the prior mean and \mathbf{C} which is the prior covariance of the dependent variable (i.e. the output). Finally, \mathcal{W} is the marginal prior on covariance matrices, which has an inverse-Wishart distribution with \mathbf{W} and n . More precisely, the distributions are:

$$\begin{aligned} \mathcal{N}(\mathbf{A}_i \mid \mathbf{M}, \mathbf{C}, \mathbf{V}) &\propto e^{-\frac{1}{2} \text{tr}[(\mathbf{A}_i - \mathbf{M})^\top \mathbf{V}^{-1} (\mathbf{A}_i - \mathbf{M}) \mathbf{C}]} \\ \mathcal{W}(\mathbf{V} \mid \mathbf{W}, n) &\propto |\mathbf{V}^{-1} \mathbf{W} / 2|^{n/2} e^{-\frac{1}{2} \text{tr}(\mathbf{V}^{-1} \mathbf{W})}. \end{aligned}$$

Essentially, the model is an extension of the univariate Bayesian linear regression model (see for example [18]) to the multivariate case via vectorisation of the mean matrix. Since the prior² is conjugate, it is relatively simple to calculate posterior values of the parameters after each observation.

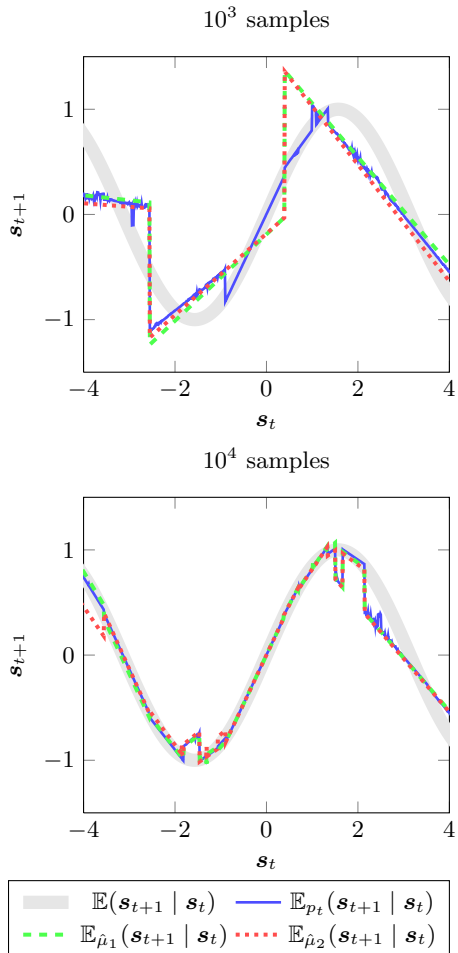


Figure 2: Regression illustration. We plot the expected value for the real distribution, the marginal, as well as two sampled models $\hat{\mu}_1, \hat{\mu}_2 \sim p_t(\mu)$.

To integrate this with inference in the tree, we need to define the marginal distribution used in (2.4). This

²We note that we use the same prior parameters $(\mathbf{M}_i, \mathbf{C}_i, \mathbf{W}_i, n_i)$ for all contexts in the tree.

is given by a multivariate Student- t distribution, so if the posterior parameters for context i at time t are $(\mathbf{M}_i^t, \mathbf{C}_i^t, \mathbf{W}_i^t, n_i^t)$, then this is:

$$p_t(\mathbf{s}_{t+1} \mid \mathbf{x}_t = \mathbf{x}, c_t = i) = \text{Student}(\mathbf{M}_i^t, \mathbf{W}_i^t / z_i^t, 1 + n_i^t), \quad (2.10)$$

where $z_i^t = 1 - \mathbf{x}^\top (\mathbf{C}_i^t + \mathbf{x}\mathbf{x}^\top)^{-1} \mathbf{x}$.

An illustration of inference using this tree is given in Fig. 2, where the piecewise-linear structure is evident. The \mathbf{s}_t variates are drawn uniformly in the displayed interval, while \mathbf{s}_{t+1} is drawn from a normal distribution with mean $\sin(\mathbf{s}_t)$. The plot shows the marginal expectation \mathbb{E}_{p_t} , as well as the expectation from two different models sampled from the posterior $p_t(\mu)$.

2.4 Thompson sampling

While estimating the Bayes-expected utility itself is a difficult problem, many exact and approximate algorithms exist for estimating the expected utility of a specific MDP μ . So, a simple idea is to take a number of samples μ_i from the current posterior distribution and then calculate the expected utility of each, in order to approximate the expected utility.

$$\mathbb{E}_p^\pi U \approx \frac{1}{K} \sum_{i=1}^K \mathbb{E}_{\mu_i}^\pi U, \quad \mu_i \sim p_t(\mu). \quad (2.11)$$

We consider only the special case $K = 1$, i.e. when we only sample a single MDP. This method, called *Thompson sampling*, was first employed in the context of reinforcement learning by [38].

Each model μ sampled from the posterior corresponds to a particular choice of tree parameters. Sampling from the posterior distribution involves two steps. The first is sampling a particular partition from the tree distribution and the second sampling a particular set of linear models for each context in the partition.

The first step is straightforward. We only need to sample a set of weights $\hat{w}_i \in \{0, 1\}$ such that $\mathbb{P}(\hat{w}_i = 1) = w_{i,t}$, as shown in [21, Rem. 2]. This creates a *partition*, with one Bayesian multi-variate linear model responsible for each context in the partition.

The second step is to sample a design and covariance matrix pair $(\hat{\mathbf{A}}_i, \hat{\mathbf{V}}_i)$ for each context i in the partition. This avoids sampling these matrices for models not part of the sampled tree. As the model suggests, we can first sample the noise covariance by plugging the posterior parameters in (2.9) to obtain $\hat{\mathbf{V}}_i$. Sampling from this distribution can be done efficiently using the algorithm suggested by [36]. We then plug in $\hat{\mathbf{V}}_i$ into the conditional design matrix posterior (2.8) to obtain a design matrix $\hat{\mathbf{A}}_i$ by sampling from the resulting matrix-normal distribution.

Thus, the final MDP sample μ from the posterior has two elements. Firstly, a set of contexts $\hat{C}^\mu \subset \bigcup_{a \in \mathcal{A}} \hat{\mathcal{T}}_a$, from all action trees. This set is a partition with associated mapping $f^\mu : \mathcal{S} \times \mathcal{A} \rightarrow \hat{C}^\mu$. Secondly, a set of associated design and covariance matrices $\{(A_i^\mu, V_i^\mu) \mid i \in \hat{C}^\mu\}$ for each context. Then the prediction of the sampled MDP is simply

$$P_\mu(\mathbf{s}_{t+1} \mid \mathbf{s}_t, a_t) = \mathcal{N}(A_{f(\mathbf{s}_t, t)}^\mu \mathbf{s}_t, V_{f(\mathbf{s}_t, t)}^\mu). \quad (2.12)$$

2.5 Approximate dynamic programming (ADP) step

Given a sample model μ , we wish to calculate an optimal policy $\pi^*(\mu)$ for it. Consider the *value function* $V_\mu^\pi : \mathcal{S} \rightarrow \mathbb{R}$, defined as:

$$V_\mu^\pi(\mathbf{s}) \triangleq \mathbb{E}_\mu^\pi(U \mid \mathbf{s}_t = \mathbf{s}). \quad (2.13)$$

Unfortunately, for continuous \mathcal{S} finding an optimal policy requires approximations. A common approach is to make use of the fact that:

$$V_\mu^\pi(\mathbf{s}) = \rho(\mathbf{s}) + \gamma \int_{\mathcal{S}} V_\mu^\pi(\mathbf{s}') dP_\mu^\pi(\mathbf{s}' \mid \mathbf{s}), \quad (2.14)$$

where we assume for simplicity that $\rho(\mathbf{s})$ is the reward obtained at state \mathbf{s} and P_μ^π is the transition kernel on \mathcal{S} induced by μ, π . We then select a parametric family $v_\omega : \mathcal{S} \rightarrow \mathbb{R}$ with parameter $\omega \in \Omega$ and minimise:

$$h(\omega) + \int_{\mathcal{S}} \|v_\omega(\mathbf{s}) - \rho(\mathbf{s}) - \gamma \int_{\mathcal{S}} v_\omega(\mathbf{s}') d\hat{P}_\mu^\pi(\mathbf{s}' \mid \mathbf{s})\| d\chi(\mathbf{s}), \quad (2.15)$$

where h is a regularisation term, χ is an appropriate measure on \mathcal{S} and \hat{P} is an empirical estimate of the

transition kernel. As we can take an arbitrary number of trajectories from μ, π , this can be as accurate as our computational capacity allows.

In practice, we minimise (2.15) with a generalised linear model (defined on an appropriate basis) for v_ω while χ need only be positive on a set of representative states. Specifically, we employ a variant of the least-squares policy iteration (LSPI [30]) algorithm, using the least-squares temporal differences (LSTD [12]) for the minimisation of (2.15). Then the norm is the euclidean norm and the regularisation term is $h(\omega) = \lambda \|\omega\|$. In order to estimate the inner integral, we take $K_L \geq 1$ samples from the model so that

$$\hat{P}_\mu^\pi(\mathbf{s}' | \mathbf{s}) = \frac{1}{K_L} \sum_{i=1}^{K_L} \mathbb{I}\{\mathbf{s}_{t+1}^i = \mathbf{s} | \mathbf{s}_t^i = \mathbf{s}\}, \quad (2.16)$$

$$\mathbf{s}_{t+1}^i | \mathbf{s}_t^i = \mathbf{s} \sim P_\mu^\pi(\mathbf{s}' | \mathbf{s}),$$

where $\mathbb{I}\{\cdot\}$ is an indicator function and where $P_\mu^\pi(\mathbf{s}' | \mathbf{s}) = P^\mu(\mathbf{s}' | \mathbf{s}, a)\pi(a | \mathbf{s})$ is decomposable in known terms. Equation (2.16) is also used for action selection in order to calculate:

$$q_\omega(\mathbf{s}, a) \triangleq \rho(\mathbf{s}) + \gamma \int_{\mathcal{S}} v_\omega(\mathbf{s}') d\hat{P}_\mu^\pi(\mathbf{s}' | \mathbf{s}) \quad (2.17)$$

This may add a small amount of additional stochasticity to action selection, which can be reduced³ by increasing K_L .

We optimise the policy by approximate policy iteration [9]. At the j -th iteration, we obtain an improved policy $\hat{\pi}_j(a | \mathbf{s}) \propto \mathbb{P}[a \in \arg \max_{a' \in \mathcal{A}} q_{\omega_{j-1}}(\mathbf{s}, a')]$ from ω_{j-1} and then estimate ω_j for the new policy.

2.6 Q-learning

One simpler idea is to use a discrete value function approximation. This can be done by sampling a set of trees (one for each action). Then, each state-action pair (\mathbf{s}, a) maps to a tree node $i = f(\mathbf{s}, a)$. We can now perform stochastic value iteration with state aggregation (see [8] for an overview). The resulting is

³We remind the reader that Thompson sampling itself results in considerable exploration by sampling an MDP from the posterior. Thus, additional randomness may be detrimental.

similar to simulation-based Q -learning, where transitions are sampled from the model.

Algorithm 2 Q -CTBRL: Q -learning for CTBRL

```

input  $\mu, \chi, \mathbf{q}, \phi$ 
for  $k = 1, \dots$ , do
   $(\mathbf{s}, a) \sim \chi$  // sample state-action
   $\mathbf{s}' \sim P_\mu(\mathbf{s}_{t+1} | \mathbf{s}_t = \mathbf{s}, a_t = a)$  // generate
  next state
   $q' = \max_{a' \in \mathcal{A}} q[f^\mu(\mathbf{s}', a')]$  // get next
  q-value
   $q[f^\mu(\mathbf{s}, a)] = (1 - \eta_k)q[f^\mu(\mathbf{s}, a)] + \eta_k(q' + \rho(\mathbf{s}, a))$ 
  // update
end for

```

Algorithm 2 gives an overview of the algorithm. The value iteration is performed on a vector \mathbf{q} , such that each context i corresponds to an approximate value q_i . The stochasticity is due to the fact that we sample state-action pairs according to some arbitrary distribution χ , which is a hyper-parameter of the algorithm, while the next state is sampled from the generated MDP μ . A final hyper-parameter is the step size sequence η_k . In practice, we can run only one iteration of Algorithm 2, with (\mathbf{s}, a) being simply the current state-action pair (\mathbf{s}_t, a_t) and $\mathbf{s}' = \mathbf{s}_{t+1}$, the next observed state.

2.7 Complexity

We now analyse the computational complexity of our approach. We look at both the online complexity of inference and decision making, as well of the API step.

Corollary 2.1. *Cover tree construction from t observations takes $O(t \ln t)$ operations.*

Proof. In the cover tree, node insertion and query are $O(\ln t)$ [10, Theorems 5, 6]. Then note that $\sum_{k=1}^t \ln k \leq \int_1^t \ln x dx \leq t \ln t$. \square

Lemma 2.1. *If $\mathcal{S} \subset \mathbb{R}^m$, then inference at time step t has complexity $O(m^3 \ln t)$.*

Proof. At every step, we must perform inference on a number of nodes equal to the length of the path

containing the current observation. This is bounded by the depth of the tree, which is in turn bounded by $O(\ln t)$ from [10, Lem. 4.3]. Calculating (2.4) is linear in the depth. For each node, however, we must update the linear-Bayesian model, and calculate the marginal distribution. Each requires inverting an $m \times m$ matrix, which has complexity $O(m^3)$. \square

Lemma 2.2. *If the LSTD basis has dimensionality m_L , then taking a decision at time t has complexity $O(K_L m_L \ln t)$.*

Proof. To take a decision we merely need to search in each action tree to find a corresponding path. This takes $O(\ln t)$ time for each tree. After Thompson sampling, there will only be one linear model for each action tree. We then need to estimate (2.16), which takes K_L operations, and requires the inner product of two m_L -dimensional vectors. \square

The above lemmas give the following result:

Theorem 2.1. *At time t , the online complexity of CTBRL is $O((m^3 + K_L m_L) \ln t)$.*

We now examine the complexity of finding a policy.

Lemma 2.3. *Thompson sampling at time t is $O(tm^3)$.*

Proof. In the worst case, our sampled tree will contain all the leaf nodes of the reduced tree, which are $O(t)$. For each sampled node, the most complex operation is Wishart generation, which is $O(m^3)$ [36]. \square

Lemma 2.4. *If we use n_s samples for LSTD estimation and the basis dimensionality is m_L , this step has complexity $O(m_L^3 + n_s(m_L^2 + K_L m_L \ln t))$.*

Proof. For each sample we must take a decision according to the last policy, which requires $O(K_L m_L \ln t)$ as shown previously. We also need to update two matrices (see [11]), which is $O(m_L^2)$. So, $O(n_s(m_L^2 + K_L m_L \ln t))$ computations must be performed for the total number of the selected samples. Since LSTD requires an $m_L \times m_L$ matrix inversion, with complexity $O(m_L^3)$, we obtain the final result. \square

From Lemmas 2.2 and 2.4 it follows that:

Theorem 2.2. *If we employ API with K_A iterations, the total complexity of calculating a new policy is $O(tm^3 + K_A(m_L^3 + n_s(m_L^2 + K_L m_L \ln t)))$.*

Thus, while the online complexity of CTBRL is only logarithmic in t , there is a substantial cost when calculating a new policy. This is only partially due to the complexity of sampling a model, which is manageable when the state space has small dimensionality. Most of the computational effort is taken by the API procedure, at least as long as $t < (m_L / \dim)^3$.

3 Experiments

We conducted two sets of experiments to analyze the offline and the online performance. We compared CTBRL with the well-known least square policy iteration (LSPI) algorithm [30] for the offline case, as well as an online variant [15] for the online case. We used one preliminary run and guidance from the literature to make an initial selection of possible hyper-parameters, such as the number of samples and the features used for LSTD and LSTD-Q. We subsequently used 10 runs to select a single hyper-parameter combination for each algorithm-domain pair. The final evaluation was done over an independent set of 100 runs.

As we had the liberty to draw an arbitrary number of trajectories for the value function estimation, we drew 1-step transitions from a set of 3000 uniformly drawn states from the *sampled* model. We used 25 API iterations on this data.

For the offline performance evaluation, we first drew rollouts from $k = \{50, 100, \dots, 1000\}$ states drawn from the *true environment's* starting distribution, using a uniformly random policy. The maximum horizon of each rollout was set equal to 40. The collected data was then fed to each algorithm in order to produce a policy. This policy was evaluated over 1000 rollouts on the environment.

In the online case, we simply use the last policy calculated by each algorithm at the end of the last episode, so there is no separate learning and evaluation phase. This means that efficient exploration must be performed. For CTBRL, this is done using Thompson sampling. For online-LSPI, we followed

the approach of [15], who adopts an ϵ -greedy exploration scheme with an exponentially decaying schedule $\epsilon_t = \epsilon_d^t$, with $\epsilon_0 = 1$. In preliminary experiments, we found $\epsilon_d = 0.997$ to be a reasonable compromise. We compared the algorithms online for 1000 episodes.

3.1 Domains

We consider two well-known continuous state, discrete-action, episodic domains. The first is the inverted pendulum domain and the second is the mountain car domain.

3.1.1 Inverted pendulum

The goal in this domain, is to balance a pendulum by applying forces of a mixed magnitude (50 Newtons). The state space consists of two continuous variables, the vertical angle and the angular velocity of the pendulum. There are three actions: no force, left force or right force. A zero reward is received at each time step except in the case where the pendulum falls. In this case, a negative (-1) reward is given and a new episode begins. An episode also ends with 0 reward after 3000 steps, after which we consider that the pendulum is successfully balanced. Each episode starts by setting the pendulum in a perturbed state close to the equilibrium point. More information about the specific dynamics can be found at [30]. The discount factor γ was 0.95. The basis we used for LSTD/LSPI, was equidistant 3×3 grid of RBFs over the state space following the suggestions of [30]. This was replicated for each action for the LSTD- Q algorithm used in LSPI.

3.1.2 Mountain car

The aim in this domain is to drive an underpowered car to the top of a hill. Two continuous variables characterise the vehicle state in the domain, its position and its velocity. The objective is to drive an underpowered vehicle up a steep valley from a randomly selected position to the right hilltop (at position > 0.5) within 1000 steps. There are three actions: forward, reverse and zero throttle. The received reward is -1 except in the case where the tar-

get is reached (zero reward). At the beginning of each rollout, the vehicle is positioned to a new state, with the position and the velocity uniformly randomly selected. The discount factor is set to $\gamma = 0.999$. An equidistant 4×4 grid of RBFs over the state space plus a constant term is selected for LSTD and LSPI.

3.2 Results

In our results, we show the average performance in terms of number of steps of each method, averaged over 100 runs. For each average, we also plot the 95% confidence interval for the accuracy of the mean estimate with error bars. In addition, we show the 90% percentile region of the runs, in order to indicate inter-run variability in performance.

Figure 3(a) shows the results of the experiments in the *offline* case. For the *mountain car*, it is clear that CTBRL is significantly more stable than LSPI, though the latter has better asymptotic performance. For the *pendulum* domain, the performance of CTBRL is almost perfect, as it needs only fifty rollouts in order to discover the optimal policy. While LSPI manages to find the optimal policy frequently, nevertheless around 5% of its runs fail.

Figure 3(b) shows the results of the experiments in the *online* case. For the *mountain car*, CTBRL managed to find an excellent policy in the vast majority of runs, and its mean performance was significantly better than that of LSPI. In the *pendulum* domain, the performance difference is even more impressive, since CTBRL reaches near optimal performance with an order of magnitude fewer episodes than LSPI, while the latter remains unstable. The main characteristic of the CTBRL is its inherent exploration ability as well as its consistency.

The success of CTBRL over LSPI can be attributed to a number of reasons. Firstly, it could be the *more efficient exploration*. Indeed, in the offline results for the mountain car domain, where the starting state distribution is uniform, and all methods have the same data, we can see that LSPI is much more consistent. The quality of the CTBRL exploration is evident in the online results, where the performance is even better than that of the offline results. CTBRL also makes *better use of the data*, since it creates an

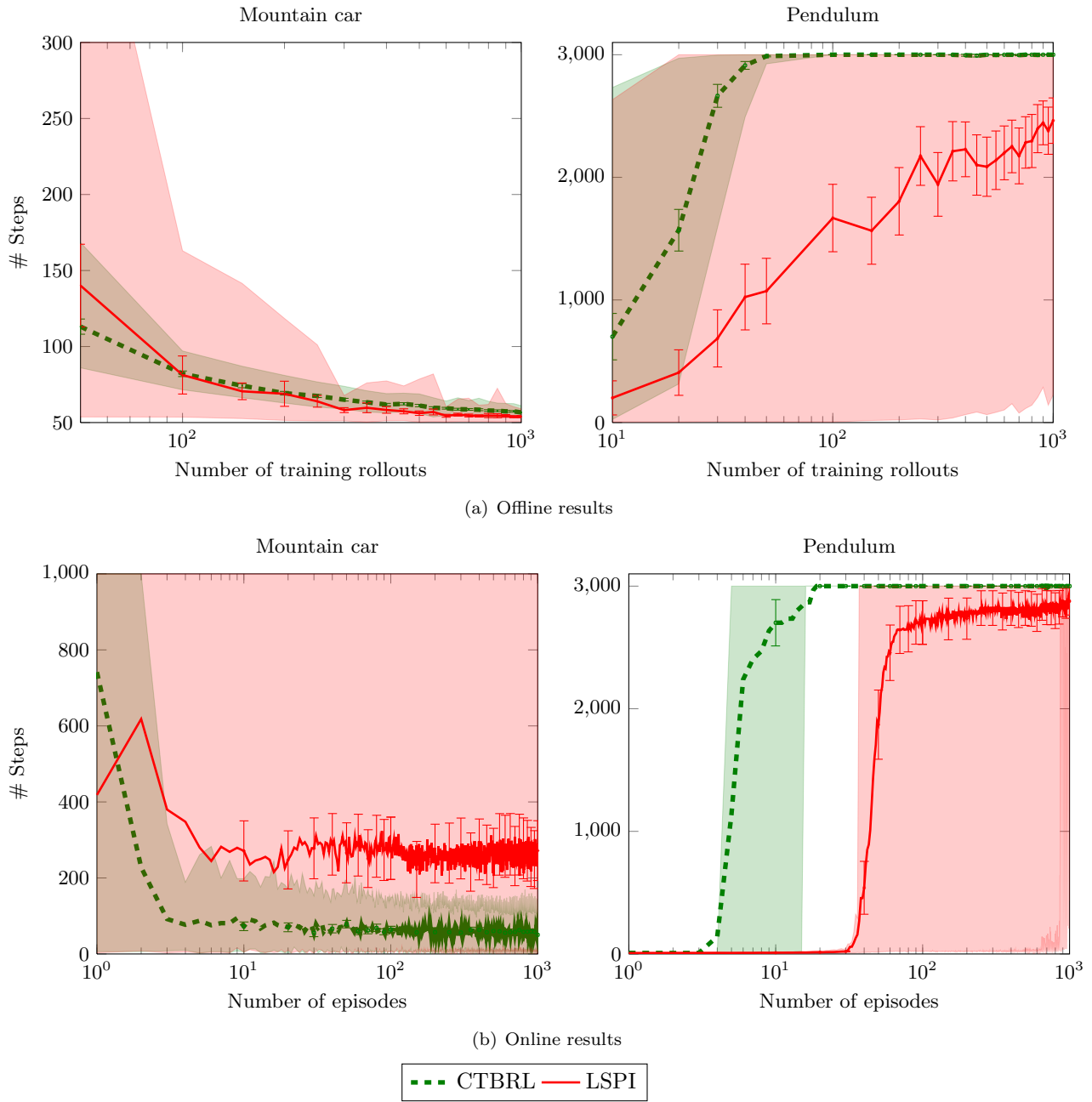


Figure 3: Experimental evaluation. The thick dotted line shows CTBRL, while the solid line shows LSPI. The error bars denote 95% confidence intervals, while the shaded regions denote 90% percentile performance across runs. In all cases, CTBRL is quicker to converge and is significantly more stable.

explicit model. This is supported by the offline results, where both CTBRL and LSPI use the same set of example trajectories and yet CTBRL is at least as good as LSPI.

4 Conclusion

We proposed a computationally efficient Bayesian approach for the exact inference of unknown dynamics in continuous state spaces. Unlike other non-parametric models such as Gaussian processes, CTBRL scales almost linearly $O(t \ln t)$ with time t , rendering suitable for online application. We combined this approach with Thompson sampling, in order to obtain good exploration policies in unknown environments. In a comparison with the well-known LSPI algorithm, CTBRL can discover significantly better policies from the same dataset. However, CTBRL is particularly good in online settings, where the exact inference, combined with the efficient exploration provided by Thompson sampling give it an additional advantage. We thus believe that CTBRL is a method that is well-suited for exploration in unknown continuous state problems.

The main drawback of our approach is the fact that ADP must be performed on the sampled models in order to obtain an improved policy. While this can be performed in the background while inference is taking place, and although we seed the ADP with the previous solution, one would ideally like to use a more incremental approach for that purpose. One interesting idea would be to employ a gradient approach in a similar vein to Deisenroth and Rasmussen [19].

Another direction of future work is to consider other sophisticated exploration policies, particularly for larger problems. Finally, it would be interesting to examine continuous actions. These can be handled efficiently both by the cover tree and the local linear models. While optimising over a continuous action space is challenging, efficient tree search methods such as [14] may alleviate that problem.

References

- [1] P. Abbeel and A.Y. Ng. Exploration and apprenticeship learning in reinforcement learning. In *Proceedings of the 22nd international conference on Machine learning (ICML 2005)*, 2005.
- [2] S. Agrawal and N. Goyal. Analysis of Thompson sampling for the multi-armed bandit problem. In *COLT 2012*, 2012.
- [3] M. Alvarez, D. Luengo-Garcia, M. Titsias, and N. Lawrence. Efficient multioutput gaussian processes through variational inducing kernels. 2011.
- [4] M. Araya, V. Thomas, O. Buffet, et al. Near-optimal BRL using optimistic local transitions. In *ICML*, 2012.
- [5] J. Asmuth, L. Li, M. L. Littman, A. Nouri, and D. Wingate. A Bayesian sampling approach to exploration in reinforcement learning. In *UAI 2009*, 2009.
- [6] R. Begleiter, R. El-Yaniv, and G. Yona. On prediction using variable order Markov models. *Journal of Artificial Intelligence Research*, pages 385–421, 2004.
- [7] D. P. Bertsekas. Dynamic programming and suboptimal control: From ADP to MPC. *Fundamental Issues in Control, European Journal of Control*, 11(4-5), 2005. From 2005 CDC, Seville, Spain.
- [8] D. P. Bertsekas and J. N. Tsitsiklis. *Neuro-Dynamic Programming*. Athena Scientific, 1996.
- [9] D.P. Bertsekas. Approximate policy iteration: A survey and some new methods. *Journal of Control Theory and Applications*, 9(3):310–335, 2011.
- [10] Aline Beygelzimer, Sham Kakade, and John Langford. Cover trees for nearest neighbor. In *ICML 2006*, 2006.

- [11] J.A. Boyan. Technical update: Least-squares temporal difference learning. *Machine Learning*, 49(2):233–246, 2002.
- [12] S.J. Bradtke and A.G. Barto. Linear least-squares algorithms for temporal difference learning. *Machine Learning*, 22(1):33–57, 1996.
- [13] E. Brunskill, B. R. Leffler, L. Li, M. L. Littman, and N. Roy. Provably efficient learning with type parametric models. *Journal of Machine Learning Research*, 10:1955–1988, 2009.
- [14] Sébastien Bubeck, Rémi Munos, Gilles Stoltz, and Csaba Szepesvári. X-armed bandits. *Journal of Machine Learning Research*, 12:1655–1695, 2011.
- [15] L. Buşoniu, D. Ernst, B. De Schutter, and R. Babuška. Online least-squares policy iteration for reinforcement learning control. In *Proceedings of the 2010 American Control Conference*, pages 486–491, 2010.
- [16] P. Castro and D. Precup. Smarter sampling in model-based Bayesian reinforcement learning. *Machine Learning and Knowledge Discovery in Databases*, pages 200–214, 2010.
- [17] M. Daswani, P. Sunehag, and M. Hutter. Feature reinforcement learning using looping suffix trees. In *Proceedings of 10th European Workshop on Reinforcement Learning (EWRL)*, 2012.
- [18] M. H. DeGroot. *Optimal Statistical Decisions*. John Wiley & Sons, 1970.
- [19] M. P. Deisenroth and C. E. Rasmussen. Pilco: A model-based and data-efficient approach to policy search. In *International conference on Machine Learning (ICML)*, Bellevue, WA, USA, July 2011.
- [20] M.P. Deisenroth, C.E. Rasmussen, and J. Peters. Gaussian process dynamic programming. *Neurocomputing*, 72(7-9):1508–1524, 2009.
- [21] C. Dimitrakakis. Bayesian variable order Markov models. In *International Conference on Artificial Intelligence and Statistics (AISTATS)*, volume 9 of *JMLR : W&CP*, pages 161–168, Chia Laguna Resort, Sardinia, Italy, 2010.
- [22] C. Dimitrakakis. Context model inference for large or partially observable MDPs. In *ICML workshop on reinforcement learning and search in very large spaces*, 2010.
- [23] Michael O’Gordon Duff. *Optimal Learning Computational Procedures for Bayes-adaptive Markov Decision Processes*. PhD thesis, University of Massachusetts at Amherst, 2002.
- [24] Y. Engel, S. Mannor, and R. Meir. Reinforcement learning with gaussian process. In *International Conference on Machine Learning*, pages 201–208, 2005.
- [25] D. Ernst, P. Geurts, and L. Wehenkel. Tree-based batch mode reinforcement learning. *Journal of Machine Learning Research*, 6:503–556, 2005.
- [26] V. F. Farias, C. C. Moallemi, B. Van Roy, and T. Weissman. Universal reinforcement learning. *IEEE Transactions on Information Theory*, 56(5):2441–2454, 2010.
- [27] T. S. Ferguson. Prior distributions on spaces of probability measures. *The Annals of Statistics*, 2(4):615–629, 1974. ISSN 00905364.
- [28] Cs. Szepesvári I. Szita. Model-based reinforcement learning with nearly tight exploration complexity bounds. In *ICML*, pages 1031–1038, 2010.
- [29] E. Kaufmann, N. Korda, and R. Munos. Thompson sampling: An optimal finite time analysis. In *ALT-2012*, 2012.
- [30] M.G. Lagoudakis and R. Parr. Least-squares policy iteration. *The Journal of Machine Learning Research*, 4:1107–1149, 2003.
- [31] M. Meila and M.I. Jordan. Learning with mixtures of trees. *The Journal of Machine Learning Research*, 1:1–48, 2001.

- [32] S.M. Paddock, F. Ruggeri, M. Lavine, and M. West. Randomized Polya tree models for nonparametric Bayesian inference. *Statistica Sinica*, 13(2):443–460, 2003.
- [33] P. Poupart, N. Vlassis, J. Hoey, and K. Regan. An analytic solution to discrete Bayesian reinforcement learning. In *ICML 2006*, pages 697–704. ACM Press New York, NY, USA, 2006.
- [34] M. L. Puterman. *Markov Decision Processes : Discrete Stochastic Dynamic Programming*. John Wiley & Sons, New Jersey, US, 2005.
- [35] C.E. Rasmussen and M. Kuss. Gaussian processes in reinforcement learning. In *Advances in Neural Information Processing Systems 16*, pages 751–759, 2004.
- [36] WB Smith and RR Hocking. Wishart variates generator, algorithm as 53. *Applied Statistics*, 21:341–345, 1972.
- [37] A. L. Strehl and M. L. Littman. Online linear regression and its application to model-based reinforcement learning. In *NIPS 2008*, 2008.
- [38] M. Strens. A Bayesian framework for reinforcement learning. In *ICML 2000*, pages 943–950, 2000.
- [39] W.R. Thompson. On the likelihood that one unknown probability exceeds another in view of the evidence of two samples. *Biometrika*, 25(3-4):285–294, 1933.
- [40] J. Veness, K.S. Ng, M. Hutter, and D. Silver. A Monte Carlo AIXI approximation. Arxiv preprint arXiv:0909.0801, 2009.
- [41] T. Wang, D. Lizotte, M. Bowling, and D. Schuurmans. Bayesian sparse sampling for on-line reward optimization. In *ICML '05*, pages 956–963, New York, NY, USA, 2005. ACM. ISBN 1-59593-180-5.
- [42] F.M.J. Willems, Y.M. Shtarkov, and T.J. Tjalkens. The context tree weighting method: basic properties. *IEEE Transactions on Information Theory*, 41(3):653–664, 1995.
- [43] W.H. Wong and L. Ma. Optional Pólya tree and Bayesian inference. *The Annals of Statistics*, 38(3):1433–1459, 2010.